Nat. Hazards Earth Syst. Sci. Discuss., 3, 4871–4917, 2015
www.nat-hazards-earth-syst-sci-discuss.net/3/4871/2015/
doi:10.5194/nhessd-3-4871-2015

Natural Hazards and Earth System Sciences
Discussions

Landslide inventory development in a data sparse region: spatial and temporal characteristics of landslides in Papua New Guinea

J. C. Robbins[1] and M. G. Petterson[2]

[1]Met Office, Fitzroy Road, Exeter, Devon, UK
[2]Secretariat of the Pacific Community, Suva, Fiji

Received: 15 July 2015 – Accepted: 16 July 2015 – Published: 17 August 2015

Correspondence to: J. C. Robbins (joanne.robbins@metoffice.gov.uk)

Published by Copernicus Publications on behalf of the European Geosciences Union.

Abstract

In Papua New Guinea (PNG) earthquakes and rainfall events form the dominant trigger mechanisms capable of generating many landslides. Large volume and high density landsliding can result in significant socio-economic impacts, which are felt particularly strongly in the largely subsistence-orientated communities which reside in the most susceptible areas of the country. As PNG has undergone rapid development and increased external investment from mining and other companies, population and settled areas have increased, hence the potential for damage from landslides has also increased. Information on the spatial and temporal distribution of landslides, at a regional-scale, is critical for developing landslide hazard maps and for planning, sustainable development and decision making. This study describes the methods used to produce the first, country-wide landslide inventory for PNG and analyses of landslide events which occurred between 1970 and 2013. The findings illustrate that there is a strong climatic control on landslide-triggering events and that the majority (~ 61 %) of landslides in the PNG landslide inventory are initiated by rainfall related triggers. There is also large year to year variability in the annual occurrence of landslide events and this is related to the phase of El Niño Southern Oscillation (ENSO) and mesoscale rainfall variability. Landslide-triggering events occur during the north-westerly monsoon season during all phases of ENSO, but less landslide-triggering events are observed during drier season months (May to October) during El Niño phases, than either La Niña or ENSO neutral periods. This analysis has identified landslide hazard hotspots and relationships between landslide occurrence and rainfall climatology and this information can prove to be very valuable in the assessment of trends and future behaviour, which can be useful for policy makers and planners.

1 Introduction

Papua New Guinea (PNG) is particularly prone to landslides due its geomorphology, climate and geology. In recent years there have been numerous landslides which have resulted in large numbers of fatalities and caused significant socio-economic impacts upon communities surrounding the landslide site and further afield (e.g. Tumbi Landslide in Southern Highlands Province; Robbins et al., 2013). Although PNG has experienced some of largest recorded landslides in the world (e.g. Kaiapit Landslide in 1988, Peart, 1991a; Drechsler et al., 1989, and the Bairaman Landslide in 1985, King and Loveday, 1985), research has tended to focus on basin scale landsliding and has largely involved documenting the characteristics of individual landslides or a cluster of landslides associated with a specific trigger mechanism (Greenbaum et al., 1995). There have been field investigations to map landslide scars in particularly sensitive regions of the country, such as along the Highlands Highway (Tutton and Kuna, 1995; Kuna, 1998) and in close proximity to mining operations (Hearn, 1995; Fookes et al., 1991), but these studies have remained largely isolated and do not conform to a standard of landslide recording. To understand the temporal and spatial characteristics of landslides and their trigger mechanisms, assessments at a regional-scale are required, particularly when trying to determine trends or develop models. Development of such regional-scale inventories can prove challenging particularly in a region such as PNG, as the nature of landslides means that: (1) they frequently result in impacts over small areas compared to impacts associated with larger-scale natural hazards and (2) the areas affected by landslides are often remote and difficult to access, as well as being widely distributed relative to one another (Kirschbaum et al., 2009; Petley, 2012). Therefore, although there have been a number of fieldwork campaigns to update and extend existing geological maps in PNG, the development of regional landslide hazard maps, based on fieldwork, has proven difficult. By extension, this has limited the development of landslide inventories in the region. The aim of this study is to build-upon existing methods and approaches (Greenbaum et al., 1995; Blong, 1985) to construct

a regional landslide inventory for PNG, to improve the current knowledge and understanding of landslide occurrences and triggering factors in the region. An overview of the materials and methods used to create the inventory are provided in section two, followed by an outline of the techniques employed to reduce temporal and spatial uncertainty in the database. In section three the results of analysis conducted on the landslide entries within the database are provided, with particular emphasis placed on the spatial and temporal distributions of landslide occurrence and the relationships with spatial and temporal distributions of rainfall variability over a range of time scales (month–seasonal–annual). Discussion and conclusions are provided in sections four and five, respectively.

Study area and landslide incidence

The dominant trigger mechanisms for many landslides around the world are earthquakes (Keefer, 2002; Meunier et al., 2007) or rainfall (Iverson, 2000; Zêzere et al., 2005; Guzzetti et al., 2007). PNG is no exception to this. PNG lies within the Maritime Continent (Ramage, 1968) and is influenced by a tropical maritime climate. This is characterised by high rainfall accumulations, which alter between wetter and drier periods seasonally, and high maximum and minimum temperatures (McGregor, 1989). Rainfall variability in this region is predominantly controlled by: (1) the meridional heat transfer of the Hadley Cell and the temporal and spatial variability of the Intertropical Convergence Zone (ITCZ), (2) the zonal Walker Circulation with its variability (e.g. El Niño Southern Oscillation) and associated oceanic currents, (3) the north-westerly monsoon circulation and (4) the physiography of the region (McAlpine et al., 1983; McGregor and Niewolt, 1998; Qian, 2008). These controls can induce rainfall variability over a range of temporal and spatial scales, which in turn affects the temporal and spatial occurrence of landslide events. In addition to the meteorological complexity of the region, PNG also lies at the intersection of the large-scale collision of the north-easterly migrating Indo-Australian Plate and the westerly-shifting Pacific Plate. Between the Proterozoic and the Holocene, the region has undergone phases of igneous activity, rifting and

subsidence, followed by periods of convergence and arc-continent collision (Hill and Hall, 2003). These processes have caused significant deformation and up-lift, which has resulted in the formation of the central mainland cordillera and numerous additional mountain ranges (Finnisterre Range, Morobe Province; Adelbert Range, Madang Province; Torocelli Mountains, West Sepik Province) across the country. These ranges have elevations in excess of 4000 m a.s.l. in places. Continuing deformation and the resultant tectonic shearing causes extensive faulting and exposes much of PNG to regular moderate to high magnitude (magnitude 7 and above) earthquakes (Anton and Gibson, 2008). Earthquakes of this magnitude have resulted in wide-spread, high-density landsliding on numerous occasions (Pain and Bowler, 1973; Meunier et al., 2007). Such events are also frequently accompanied by landslide dams, which can cause significant additional damage upon breaching (King and Loveday, 1985).

The physiography of PNG (Fig. 1) means that it is affected by a significant landslide hazard, the true nature of which has been difficult to quantify due to inadequate data (Blong, 1986). However, the regularity of destructive landslide events, particularly in mining areas, has produced a number of scientific papers reviewing landslide activity. Stead (1990) provides the most comprehensive overview, by identifying, from an engineering geology perspective, the different types of landslides which have been observed across the region. These include: (1) debris slides, avalanches and flows, (2) rotational slumps, (3) mudslides and (4) translational slides and rockslides (Fig. 2). Debris slides, avalanches and flows are considered the most common and predominantly involve the soil and uppermost weathered material. They usually occur on steep slopes ($> 45^{\circ}$) of deformed rock, thinly-bedded mudstones and closely foliated metamorphic rocks and, in certain circumstances, such as in response to very high magnitude seismicity, can result in catastrophic failures (King and Loveday, 1985; Hovius et al., 1998; Ota et al., 1997).

Also common, particularly in the Papuan Fold Belt, are rotational slumps. These generally occur in homogeneous sedimentary rocks, such as mudstones, marls, sandstones and greywackes, on slopes as low as 10°. In these circumstances the displace-

ment of material is generally limited, while events occurring on steeper slopes ($> 30^{\circ}$) can result in deposits with volumes in excess of 500 000 m^3 (e.g. Dinidam Landslide; Blong, 1986). Numerous slumps, of varying size, have been observed along the Highlands Highway (Tutton and Kuna, 1995; Kuna, 1998) and can regularly lead to road closures and property damage. In addition to slumps, mudslides also result in damage and disruption, affecting both infrastructure and property, along the Highlands Highway. Defined as "masses of argillaceous, silty or very fine sandy debris" which displace material by "sliding on discrete boundary surfaces in relatively slow moving lobate forms" (Stead, 1990), they are most frequently observed in areas which are underlain by the Chim Formation. Movements of this type are particularly problematic because their generally slow displacement rate ($\sim 60\,mm\,yr^{-1}$ at Yakatabari; Blong, 1985) can increase rapidly associated with localized changes in shear strength and pore water pressure. Furthermore variations in depth, width and style of movement (Comegna et al., 2007) and the fact that they can occur on very low slope angles (between 6 and 15°), which coincide with settled and populated areas, means that they are difficult to mitigate against. By contrast, translational slides and rockslides typically occur on very steep slopes (between 30 and 50°) in areas with deeply incised terrain. The failure mechanisms of these slides are strongly influenced by bedding planes, joints, faults and the interface between weathered material and fresh bedrock. Given the highly fractured and deformed nature of many rocks in PNG these slides can occur in a wide range of geological materials. However, the distribution of translational slides and rockslides is strongly linked to the topography, making areas susceptible to them easier to identify.

2 Materials and methods

2.1 Regional landslide inventory construction: criteria, sources and structure

PNG currently has no systematic, routine approach for recording landslide events. This means that although a large number of landslides have been identified by their scars and deposits (Kuna, 1998) the dates of events are rarely recorded. To collate a landslide inventory which can be used to examine the temporal and spatial frequency of landslides and the corresponding relationship between these events and potential landslide triggers, it is essential that the dates and locations of landslides are recorded. Therefore, in the new PNG inventory only those landslides where both the date and location could be established with reasonable accuracy were entered. The precise date of landslide occurrence is often difficult to determine, however, where there are eye witnesses to the event the day of initiation can be recorded. In instances with no eye witnesses to the event, the time of initiation was approximated using a minimum and a maximum date boundary relating to the earliest and latest dates within which the landslide event occurred. The minimum and maximum dates frequently related to the start and end dates of potential landslide-triggering events, such as a flood event, which resulted in landslides. The basic location information required for a landslide to be included in the inventory was either a village or landmark name and the administrative province. All landslide records were analysed closely for the veracity and accuracy of essential data in terms of geographical locality, time, corroborating evidence (e.g. witness statements, press, quality of writing and reporting), and incident impact. Many records were dismissed as they "failed" the quality test needed for a study such as this.

Records of landslide activity were collected from a number of sources, including:

- technical reports and site inspection logs obtained from the PNG Mineral Resources Authority (MRA) and the Department of Mineral Policy and Geohazards Management archives;
- accessible journal publications;

- newspaper/media records;
- internet publications (e.g. Office for the Coordination of Humanitarian Affairs (OCHA)/ReliefWeb);
- supplementary hazard and disaster archives – e.g. Dartmouth Flood Observatory (Brackenridge, 2010; Brackenridge and Karnes, 1996); USGS National Earthquake Information Centre (NEIC); OFDA/CRED International Disaster Database (EM-DAT, Guha-Sapir and Below, 2002); Global Disaster Identifier Number (GLIDE).

Each data source used to construct the new landslide inventory had its own uncertainties and limitations and therefore the details captured for each landslide entry vary in completeness and scientific content. The most consistently available data for a landslide event were the (approximate) date of occurrence, affected areas, trigger mechanism (i.e., heavy rainfall) and the impacts of the event. Less consistently reported were the landslide type and the landslide size (volume and/or area affected). A full list of the critical and relevant information collected for each landslide entry, are shown in Table 1.

The development of a landslide database has a number of complexities. Firstly, although the majority of information sources documented individual landslides which could be spatially and temporally identified, there were a number of occasions when terms such as "some" or "numerous" were used to describe a landslide cluster, with no further spatial or temporal information related to the individual landslide deposits. In these instances, the sources often outlined the area or villages affected by the landslides but did not provide an indication of the exact number of landslides which had contributed to the observed impacts. To account for this, an additional attribute column referred to as "landslide cluster group size" was added to the database. This allowed each entry to be assigned to one of the four cluster group sizes, representing the number of landslides that were believed to have been associated with the database entry: (1) 1–10, (2) 10–100, (3) 100–1000 or (4) > 1000. Where sources indicated that landslides affected multiple villages, resulting from the same potential triggering factors,

an entry for each unique spatial location affected was included in the database. This method aims to capture some of the uncertainty around the recording of the "true" number of landslides initiated by a triggering event, while maintaining the integrity of those events which have the required temporal and spatial information necessary for analysing patterns, trends and triggering mechanisms.

Secondly, the data sources used to collate the PNG inventory are produced by a range of authors (e.g. research scientists, geologists, media correspondents and humanitarian agencies), some of whom have no specialist knowledge of documenting landslide events. This introduces inaccuracies particularly with regard to the more technical language used to document the event, such as identifying landslide type. In media publications for example, the majority of events are described using the term "landslide". In a small number of cases however, the landslides are referred to as mudflows but there is little evidence to suggest that this term reflects the Cruden and Varnes (1996) landslide classification. It should also be noted that there are potential inaccuracies where landslide triggers have been pre-determined in the media and other information sources, without a site inspection of the landslide by geotechnical specialists. In many instances the decision on which type of triggering event led to a landslide is based on the testimonies of people living within the affected community. The decision was taken to include information related to the potential trigger if it was available, regardless of the data source, as in the majority of cases the triggering events could be cross-referenced and verified, in terms of their timing and location by using multiple hazard and disaster databases. This approach meant that it was possible to provide corroborating support as to whether earthquakes, flooding or tropical cyclones could have contributed to the landslide entries recorded. Furthermore, it allowed multiple potential triggering factors to be attributed to a single database entry if the need was required. Data for other attributes, such as landslide type and size were only added where information was available from a scientific source (e.g. technical site reports or journal publications).

2.2 Reducing spatial and temporal uncertainty in the landslide inventory

The variety of data sources used to collate the landslide inventory introduced a number of spatial and temporal uncertainties. For example, spatial information relating to landslide activity was often provided by the name of a town, village or landmark which had been impacted by the event, rather than the latitude and longitude of the landslide head scarp or deposit. Some of these locations were found to be some distance from the actual landslide site, while in other cases village names were misspelt or had changed over time making them difficult to spatially identify. To address the issue of spatial uncertainty a number of steps were taken:

1. Landslide entries were cross-referenced against recent settlement data provided by the PNG MRA. This allowed the correct province and administrative district to be identified in the majority of cases. It was also possible to check whether the settlement had any other names associated with it, or varieties of spelling.

2. Where possible static maps found in journal publications and site inspection reports were digitized to provide information on the size and location of the landslide deposit or identify a geographical area affected by landsliding. This was particularly useful for identifying the locations or areas affected by earthquake-induced landsliding. In a number of cases, areal extents of high-density landsliding associated with a specific earthquake epicentre could be identified and mapped.

3. Landslide entries were also cross-referenced with 30 m False Colour Composite (FCC) Landsat satellite images (Vohora and Donoghue, 2004; Petley et al., 2002), a technique which has proven successful for identifying landslide scars in PNG and globally (Greenbaum et al., 1995). Using the terrain-, radiometrically- and geographically-corrected Landsat images available from the Earth Resources Observation and Science (EROS) data centre, FCC images were produced using bands 4 (near infrared; reflected 0.75–0.9 µm), 5 (mid-infrared; reflected 1.55–175 µm) and 7 (mid-infrared; reflected 2.08–2.35 µm) where bare rock (dark blue

tones), which become exposed following landslides, can be differentiated from vegetated slopes (variations of red tones). FCC images were then overlain on digital terrain and settlement data so that the location and, where possible, size of the landslide(s) could be verified (Fig. 3). In order to confirm that the blue tones observed in the FCC images were associated with landslide scars, the Digital Number (DN) values of the 7 bands were extracted from the area identified as a landslide scar and compared against the typical spectral ranges indicative of many active landslides (Table 2; Petley, 2002). If the values corresponded well, then the landslide entry was considered spatially verified. Although this method proved useful for a number of the landslide entries, cloud cover and shadowing prevented other landslide entries being verified with this technique. Furthermore landslides with widths or lengths smaller than 50 m could not be captured, due to the resolution of Landsat images (Petley, 2002).

Quantifying spatial uncertainty is particularly challenging where a wide variety of data sources have been used to collate the landslide inventory, as in this case. Therefore in this study, each entry is assigned to a spatial uncertainty group based on a more subjective decision framework. The "low uncertainty" group represents entries which were digitized based on information from journal publications and/or site inspection reports and the satellite-based FCC method. Other entries included in this group, were those where latitude and longitude information of the landslide site (i.e. the location of the landslide deposit) were available. The "medium uncertainty" group represents entries where the village or landmark affected was identified and successfully cross-referenced with MRA settlement data so that a latitude and longitude for the affected site(s) was identified. The "high uncertainty" group represents entries where only an approximate area, such as the river catchment or Local Level Government (LLG) area could be identified. In these instances an approximate latitude and longitude point representative of the catchment or LLG area were recorded in the database. In the case of earthquake-induced landsliding, where information on the location of landslides was scarce, the earthquake epicentre or a point representative of the area of high density landsliding was recorded. In both cases these entries were assigned to the "high uncertainty" group.

In addition to spatial uncertainty, the availability of temporal information varied significantly depending on the data source used to identify the landslide. For very large or high-density landslides which resulted in large socio-economic impacts, the dates when landslides occurred were often clearly recorded in either site inspection reports or scientific journal publications. However where landslides were identified as a secondary natural hazard, occurring as a result of flooding or an earthquake, the dates of associated landslides were poorly recorded. In these instances, landslide initiation dates could only be estimated based on the date of the earthquake or the period over which flooding was recorded. For these events, the estimated time of landslide initiation was constrained between a minimum and maximum date boundary. This was accomplished by cross-referencing the date and potential landslide trigger against multiple hazard and disaster databases. For flood induced landslides, the Dartmouth Flood Observatory archive (Brakenridge, 2010) was particularly useful, as it compiles flood inundation extents and additional impact information, including secondary hazards such as landslides. This information has been collected since 1985 using news, governmental, instrumental and remote sensing sources. For earthquake-induced landslides, the PNG Geophysical Observatory and the USGS PAGER (Prompt Assessment of Global Earthquakes for Response) databases were used. Using information from the multiple hazard and disaster databases two distinct fields were added to the inventory: a start and end date boundary, holding information on the day, month and year in each case, relating to the earliest and latest possible date, respectively, when landslides could have been initiated. By carefully cross-referencing each landslide entry, the uncertainty around the time and duration of each potential triggering-event was reduced. For 80 % of entries, the time over which landslides were likely to have been initiation could be constrained within a period of 10 days or less. For the remaining 20 % of entries, triggering event durations exceeded 10 days. For 9 % of those entries, the duration of

the triggering events exceeded 30 days which means that landslides could have been initiated or been active at any point over this period.

2.3 Rainfall data

Unfortunately at the time of this analysis rainfall gauge data were not available from the National Weather Service in PNG. However, gauge-based climatology data (monthly means over various reference periods) were available for nine sites across PNG via the World Meteorological Organisation (WMO) website (Fig. 1), while monthly rainfall data were available for an additional two sites via direct correspondence with mining companies. A major drawback of these data is their sparse number and spatial distribution. Eight of the eleven rainfall gauge sites are located in coastal areas, with only three sites representing rainfall patterns in areas known to experience the majority of landslides. Furthermore, the WMO gauge data were only available as climatological averages and therefore could not provide an indication of the temporal variability of rainfall at different timescales. Given the limitations of the available rainfall gauge data, additional sources of rainfall data were sought. These additional data were obtained from the Global Precipitation Climatology Centre (GPCC). The GPCC Full Data Reanalysis Product Version 6 (Adler et al., 2003) uses near-real-time and non-real-time gauge stations held in the GPCC database to produce gridded (0.5° or ∼ 55 km resolution) monthly rainfall accumulations over land areas, around the globe. WMO and other rainfall gauge-based data sources are interpolated to produce the gridded datasets, offering greater temporal and spatial resolution for better comparisons between rainfall and landslide occurrences.

Monthly rainfall accumulations were not available for the entire period of the landslide inventory (1970–2013) and therefore, monthly data over the period 1970 to 2010 (41 years) have been used to form the basis of the climatological analysis in this study. To compare the spatial and temporal characteristics of landslide activity relative to changing rainfall patterns, climatological analysis has focused on only those GPCC grid squares within which landslide activity has been recorded over the duration of

the PNG landslide inventory. This resulted in monthly rainfall totals from 53 GPCC grid squares being used to generate a monthly rainfall climatology, a range (90th percentile to 10th percentile) of area-averaged, monthly rainfall percentiles (based on the 41 year reference period) and annual rainfall accumulations. In order to assess the time series characteristics of the 41 year rainfall record, 6-monthly rainfall totals for May to October and November to April were calculated for each of the 53 GPCC grid squares. These two periods correspond to south-easterly trade flows being dominant and north-westerly monsoon flows being dominant across PNG, respectively. Using these 6-monthly totals, a standardized rainfall anomaly index (RAI) was calculated for each of the 53 GPCC grid squares using:

$$X'_{ij} = \frac{X_{ij} - \overline{X}_i}{S_i} \quad (1)$$

where X'_{ij} is the standardized 6-monthly rainfall total for GPCC grid square i and 6-monthly period j, X_{ij} is the corresponding 6-monthly rainfall total, $\overline{X}_i$ is the mean 6-monthly rainfall total for GPCC grid square i calculated over the period 1970 to 2010, and S_i is the standard deviation of the 6-monthly rainfall total calculated over the same reference period.

A landslide-area, rainfall anomaly index was then calculated by averaging over all of the 53 GPCC grid squares representing the landslide affected areas in PNG as follows:

$$\mathrm{RAI} = \frac{1}{n}\sum_i X'_{ij} \quad (2)$$

where RAI is the area-averaged value for 6-monthly period j and n is the number of GPCC grid squares.

The availability of gridded GPCC data means that in addition to analysing the temporal variability of rainfall and landslides, the spatial characteristics of rainfall and their link to landslide occurrence can also be investigated. Gridded maps of mean annual

precipitation (MAP) and 3-monthly seasonal mean precipitation maps, as calculated from monthly data over the 1970–2010 reference period, have also been produced so that rainfall distributions can be reviewed relative to landslide affected locations.

3 Results

3.1 Landslide inventory statistics

The database consists of 167 entries recorded between January 1970 and December 2013. Each entry represents a single landslide occurrence or a cluster of landslides, identifiable by a unique spatial location. The spatial locations of individual landslides or clusters of landslides are provided by latitude and longitude points, which are additionally assigned to a spatial uncertainty group (low, medium and high). The majority (~ 63 %) of entries are in the medium spatial uncertainty group, representing entries where latitude and longitude information for the affected village or landmark associated with the landslide(s) has been successfully cross-referenced with MRA settlement data. In these instances, the landslide or landslide cluster is expected to be within 10 km of the village/landmark identified in the source material. Approximately 10 and 26 % of entries fall into the high uncertainty and low uncertainty groups, respectively. The landslides collected in the database tend to represent large-scale, high- to medium-impact events. The magnitude of the landslide events has been assessed predominantly on the impacts the event had upon the community, as this information was more readily available than quantitative size (volume or area) information. 61 % of entries had impact information available for analysis and 38 % of these can be categorized as high-impact landslide events which resulted in fatalities and additional damage to infrastructure. Medium impact landslides, representing those where there was significant damage affecting a number of different types of infrastructure but no recorded fatalities account for 43 % of the entries where this information was available, while 19 % of entries can be categorised as low impact landslides which resulted in some minor

damage or disruption. Of course, there are instances where very large landslides do not result in extensive damage or fatalities because they occur in very sparsely populated regions. The rockslide/debris flow at the Hindenburg Wall in Western Province had an estimated volume of between 5 and 7 million m^3 (Zeriga-Alone, 2012) however there are no records of substantial damage associated with the event. By reviewing both the impact information and the volume/area data where it was available (~ 24 % of database entries), it can be asserted that the majority of the landslides or landslide clusters captured in this new inventory are large-scale, high to medium impact events.

The 167 database entries can be subdivided into landslide-triggering events. By doing this, database entries are grouped based on whether they are associated with the same potential triggering-event, identified by a unique temporal period. This is possible because multiple landslides and/or landslide clusters can occur associated with the same triggering event and can often affect more than one community across a geographical area. This means that there can be multiple database entries associated with the same temporally specific triggering event (e.g. a flood event). In this study, triggering-events are defined as external factors, such as a rainfall event or earthquake, which changes the state of the slope and results in a landslide. In the new PNG landslide inventory, the 167 entries are the result of 103 separate landslide-triggering events. The triggering-events captured within the inventory include earthquakes, flooding, tropical cyclones, monsoon rainfall and anthropogenic influences (e.g. excavations, mining). Using the cross-referencing approaches outlined in Sect. 2.2, it was possible to verify the source information and determine whether earthquakes, flooding or tropical cyclones could have contributed to the landslide occurrences in the inventory. Frequently (> 35 % of landslide-triggering events), a combination of factors were noted as being influential for initiating the landslide or landslides, while in ~ 15 % of landslide-triggering events the potential trigger was not recorded or was unknown. This was either because the triggering event could not be established, even after significant research on the event (e.g. the Kaiapit Landslide in Morobe Province in 1988; Peart, 1991a), or it was simply missing from the information source. Rainfall and the vari-

ous combinations of triggers associated with it (i.e. rainfall and anthropogenic activity or rainfall and earthquake activity), account for the majority (~ 61 %) of all landslide-triggering events in the PNG inventory (Fig. 4). This is not unexpected given that PNG experiences some of the highest annual rainfall totals globally (McAlpine et al., 1983).

In addition to rainfall associated triggers, ~ 22 % of entries were linked with earthquakes. All of the earthquakes which were identified as triggering landslides were of magnitude 5 or greater. These events are widely distributed across PNG, with events being observed through the Papuan Fold Belt tectonic seismic zone, as well as the North Sepik, Ramu, Huon, New Britain and Bougainville Island tectonic seismic zones (Ripper and Letz, 1993). It is surprising that there are not more records of earthquake-induced landsliding events in PNG, particularly given the complex nature of tectonics in the area and the regularity with which the region experiences moderate to high magnitude earthquakes (Anton and Gibson, 2008). Table 3 shows return periods, in years, associated with magnitude 6.0 earthquakes in the different seismic zones highlighted above (Ripper and Letz, 1993) and suggests that the number of earthquakes capable of triggering landslides (i.e. earthquakes greater than magnitude 5 in the PNG landslide inventory), are regular occurrences in these regions. This would suggest a discrepancy between the number of potential earthquakes capable of triggering many landslides and the number of earthquakes which are actually recorded to have resulted in landslides, in PNG. One reason for this is that in these instances, landslides are observed as secondary hazards to the principal hazardous event and such secondary hazards are frequently subject to large-scale under-reporting (Petley et al., 2007). Due to the limited number of earthquake-only, landslide-triggering events, these events, together with those earthquake/anthropogenic triggering events, will not be analysed further in this study. With regard to anthropogenic influences on landsliding, there are only a very small proportion of entries (< 5 %) where landslides are believed to have been triggered solely by anthropogenic activities. The majority of these entries are associated with infrastructure development in support of mining activities, and are usually well documented as the propensity for compensation payouts for perceived anthropogenic land-

slides has increased (Kuna, 1998). Although these events may be well documented, they are not always rigorously or independently assessed in terms of the landslide trigger factors. Therefore, given that there is significant uncertainty around anthropogenic activity as a stand-alone triggering mechanism, the decision has been made to include these entries in the further analysis. It should also be noted that 3 % of the landslide-triggering events were assigned to a category labelled "Other". These landslides were thought to be associated with lake overtopping instances (Peart, 1991b) or river erosion, either of which can be linked to periods of either high-intensity or prolonged rainfall and therefore these events will also be included in the further analysis.

Based on the assessment of the potential triggering-event information held in the PNG landslide inventory, further analysis and results focus on the 86 landslide-triggering events which are associated with rainfall, and the various combinations of triggers related with it (Fig. 4), as well as all those entries linked to the "Anthropogenic", "Other" and "Unknown" trigger factor categories.

3.2 Temporal characteristics of landslide occurrence

Analysis of the annual occurrence of the 86 landslide-triggering events indicates that there is large year to year variability (Fig. 5). There are distinct periods when the number of landslide-triggering events increases (1975–1976, 1983–1991, 2002–2009) and periods when the number of landslide-triggering events is substantially lower (1972–1973, 1981–1982, 1994–1995, 1999, 2001 and 2010–2011). There also appears to be a slight increasing trend with more landslide-triggering events being recorded near the end of the time series, particularly over the period between 2006 and 2007. A review of the temporal occurrence of recorded landslides indicates a strong climatic control on the triggering events (Fig. 5), with the highest numbers being observed between December and March, with a second peak in May. Fewer landslide-triggering events are observed between June and October, after which the number of landslide-triggering events gradually increases. This pattern of landslide activity relates closely with the periods dominated by north-westerly monsoon flows and south-easterly trade flows re-

spectively. Many locations in PNG observe drier conditions and lower monthly rainfall totals during the period between May and October when south-easterly trade winds are dominant in the region, while wetter conditions tend to prevail between November and April coinciding with the north-westerly monsoon (Figs. 1 and 5).

Despite the strong seasonality illustrated in Fig. 5, landslide-triggering events associated with rainfall, continue to be observed during the drier season. This differs from regions such as Nepal, where the number of fatal landslides fall to almost zero between November and April, which lie outside of the South Asian Summer Monsoon (Petley et al., 2007). By comparing percentiles of monthly precipitation climatology (based on the 41 year rainfall data reference period) with individual monthly rainfall totals observed at times of landslide activity, it is possible to identify why this may be the case. Landslides occurring in the drier season are, in the majority of cases (~ 61 %), associated with months which observed exceptional (> 80th percentile) rainfall (Fig. 6). This compares to the wetter season where only 44 % of entries are linked to monthly rainfall totals greater than the 80th percentile of climatology. In fact between February and May, 42 % of landslides occurred during months with rainfall totals less than the 50th percentile. This indicates that during the drier season, landslide-triggering events tend to be associated with more extreme rainfall accumulations, while during the wetter season larger numbers of landslides can be triggered during months with lower, absolute monthly rainfall totals. This may initially seem counterintuitive, as typically higher monthly rainfall totals are observed during the wetter season (Fig. 5). However, a review of the coefficient of variation (CV), calculated by dividing the standard deviation by the mean, shows that there is greater rainfall variability during the drier season (CV =~ 52 %) compared with the wetter season (CV =~ 30 %). The maximum and minimum 6-monthly rainfall total for the north-westerly monsoon season are 4782 and 490 mm, respectively, while the maximum and minimum 6-monthly rainfall total for the drier season is 5741 and 143 mm, respectively. These statistics indicate that over the landslide affected areas in PNG the wetter season is associated with more persistent, less variable rainfall which results in high average rainfall totals, while during

the drier season rainfall is less persistent and more variable, with large positive and negative departures from the mean. Relating the rainfall climatology statistics with the distribution of landslide events observed in Fig. 6, suggests two things: (1) given that the majority of landslides initiated in the drier season are linked to extreme rainfall (~ 61 %) they are likely to be associated with convective storms which are generally small, localised, and more isolated rainfall events, (2) slope instability initiated during the wetter season is likely to be associated with the greater and more persistent water availability made possible by more consistent deep convection affecting the region. Greater water availability and interaction with the surface and subsurface of slopes, allows multiple mechanisms of instability (e.g. changes in groundwater level, greater water-slope interactions associated with increased infiltration and increases in runoff and erosion) to act upon susceptible slopes to alter pore water pressures and shear strength to enhance potential instability throughout the wetter season. It also suggests that rainfall accumulated over all wetter season months may be important and influential in triggering landslides during the monsoon period, particularly where landslides are triggered during months with below average rainfall.

Figure 6 indicates that season-to-season rainfall variability could have important impacts on the number of landslide-triggering events, particularly in the drier season. To understand how this variability is related to landslide occurrence, total numbers of landslide-triggering events per 6 month period have been calculated and compared against a 6-monthly rainfall anomaly index (RAI). Figure 7 illustrates that there is considerable interseasonal rainfall variability across the grid squares affected by landslide activity. Within this variability there are groupings of positive rainfall departures (1970–1971, 1974–1978, 1983–1985, 1988–1991, 1998–2001 and 2007–2009), which indicate wetter conditions for consecutive 6-monthly periods. The grouped positive rainfall departures are seen to persist for between 2 and 5 seasons and occur at intervals of between 3 and 7 years. The average recurrence of these groupings over the 1970–2010 reference period is approximately 4.5 years. This recurrence interval is similar to the average time between El Niño Southern Oscillation (ENSO) events (McGregor

and Nieuwolt, 1998). Using the NOAA/ESRL/PSD bimonthly, ranked index of the Multivariate ENSO Index (MEI; Wolter and Timlin, 1993, 1998), years associated with the extreme modes of the southern oscillation have been identified. Based on these data, collected in 2012, Table 4 illustrates years which are associated with El Niño events and La Niña events, respectively. It is widely acknowledged that El Niño introduces "typically" drier than normal conditions to PNG (McVicar and Bierwirth, 2001) as the zone of deep convection, associated with the rising limb of the Walker Circulation, accompanies the eastward propagation of warmer sea surface temperatures (Qian et al., 2010), and that La Niña introduces "typically" wetter conditions.

Interestingly, the groupings of positive rainfall departures tend to follow, rather than coincide with, La Niña episodes in PNG (Fig. 7). Furthermore, landslide-triggering events tend to coincide with La Niña episodes or ENSO neutral episodes and are less directly coincident to the groupings of positive rainfall departures. El Niño episodes tend to coincide with seasons where none or very few landslide-triggering events occur and where large negative departures from the 6-monthly mean rainfall are observed. These departures are usually greatest in the drier season. However, landslide-triggering events continue to occur particularly during the wetter seasons of El Niño episodes (i.e. 1987 and 1992; Fig. 7). This can partially be explained by reviewing the variability of the wetter season RAI to the drier season RAI. Figure 8 shows that 6-monthly rainfall exhibits larger variability between consecutive drier seasons, compared to variability between consecutive wetter seasons. The occurrence of El Niño and La Niña events appears to have a large influence on the drier season rainfall variability, as the peaks and troughs in the drier season 3 year running mean illustrate, but limited influence on the wetter season RAI. Therefore landslide-triggering events continue to occur during the north-westerly monsoon season during all phases of ENSO, but less landslide-triggering events are observed during drier season months during El Niño phases, than either La Niña or ENSO neutral periods.

3.3 Spatial characteristics of landslide occurrence

As with the temporal variability, landslide-triggering events are very unevenly distributed spatially across PNG (Fig. 9a). Higher densities of landslide occurrences are observed in provinces which intersect the mountainous central spine of the country. The highest densities are seen in Western Highlands, Chimbu, Western, Central and West Sepik Provinces as well as in the Huon Peninsula in Morobe Province. The spatial distribution of the landslide entries appears to be determined primarily by a combination of relief, precipitation and population density. The high density pocket of landslide activity observed in northern Western Province coincides with the area of greatest annual rainfall (Fig. 9b). This zone of high rainfall accumulations extends towards the south-east as a band, following the southern edge of the Papuan Fold Belt. The area directly south of the Fold Belt, where the highest rainfall accumulations tend to be observed, is comprised of predominantly flat, swampy plains and therefore records of landslide activity are scarce in these areas. The northern edge of this band of high rainfall accumulations coincides with relief which exceeds 1000 m and this is where clusters of landslides begin to be observed, extending down the southern edge of the Papuan Fold belt in parallel with the band of high annual rainfall accumulations.

Additional high density pockets of landslide occurrence are seen in Western Highlands and Chimbu Provinces (Fig. 9a), which lie within the central mainland cordillera where annual rainfall totals exceed 2700 mm yr^{-1} and relief can exceed 3000 m in places. The terrain is very rugged and slope angles can vary significantly, up to 50°. Despite this, these areas are some of the most densely populated of the mountainous-rural provinces in PNG, increasing the likelihood for landslides to interact with communities and infrastructure and be recorded (Fig. 9c). In addition, these areas also have high percentages of total cultivated land areas compared to their total land area, with Western Highlands, Chimbu and Eastern Highlands Provinces having 50, 42 and 50 % total cultivated land areas, respectively (Saunders, 1993; Bourke and Harwood, 2009). This compares to the southern Provinces (Western, Gulf, National Capital District and

Oro) where on average less than 20 % of the total land area is cultivated (Saunders, 1993; Bourke and Harwood, 2009). Therefore in addition to higher densities of people with the potential to be affected by landslides, the populations within Western Highlands and Chimbu Provinces tend to have increased interaction with the land through agricultural practices which in turn can alter slope stability and can lead to an increased probability of landslide occurrence. Furthermore, these areas are also known to be underlain by the Chim Formation. This is comprised of dark grey, thinly laminated mudstone with siltstone and some volcaniclastic sandstone. The mudstones are generally weak and break down to form highly plastic silty clay (Peart, 1991c). Rotational landslides and mudslides are more common in areas where this formation crops-out or is overlain by limestone or unconsolidated scree deposits, as interactions with water or seismic activity can easily mobilise this weak strata.

The strong seasonality observed in the temporal analysis between rainfall climatology and landslide-triggering events can also be observed spatially, particularly during the drier season. Splitting the landslide entries into 3-monthly seasons (December, January and February (DJF); March, April and May (MAM); June, July and August (JJA); September, October and November (SON)) allows the temporal and spatial distributions of medium to large landslides to be observed (Fig. 10). Corresponding 3-monthly mean rainfall composites (based on the 41 year reference period) additionally illustrate how rainfall distribution varies spatially as the seasonal cycle progresses. It is evident that as the rainfall distribution alters so does the distribution of landslide affected areas, particularly as the cycle moves from the wetter season (DJF and MAM) to the drier season (JJA and SON). During DJF and SON, the highest rainfall totals are observed in the western-central region of Western Province, along the border with Indonesia, and along northerly-facing coastlines. The well defined rainfall pattern observed in the wet season plot in Fig. 9b starts to develop in SON, extending southeastwards from the western border region, and strengthens through DJF and MAM. Landslides are observed at the northern edge of this band, as rainfall interacts with topography in excess of 1000 m. In both the DJF and SON seasons, landslide-triggering

events are broadly confined to the central mainland cordillera and mountainous areas (north-west Toricelli Mountains and north-central Adelbert Range during DJF and south-east Owen Stanley Range on the Papuan Peninsula during SON) of the country.

Of the four seasons, the greatest spatial spread of landslide occurrences tends to occur during JJA and MMA (Fig. 10). The reasons for this are different in each case. As identified in Fig. 6, landslide-triggering events during JJA tend to be associated with exceptional rainfall which exceeds the 80th percentile for the month of initiation. Rainfall during this season is driven predominantly by orographic and physiographically-induced processes. These mesoscale features, including mesoscale convective complexes, mountain-valley winds and land–sea breezes, lead to localised, smaller-scale rainfall events affecting distinct regions of PNG (i.e. southern coast of New Britain and the north-eastern mainland region of the Huon Peninsula). The exception to this is the area in northern-Western Province, close to the border with Indonesia, which maintains moderate-to-high rainfall totals throughout the year. The dynamical processes driving rainfall appear to broadly coincide with locations which experience landslide activity at this time of year and in fact rainfall can be considered the dominant process affecting the spatial variability of landslides during this season. However, while it is possible to identify potential zones where mesoscale features may induce rainfall more regularly and by extension trigger landslides during this season, identifying actual locations of landslides cannot be determined due to the large degrees of variability inherent to this season. By comparison the large spread of landslide-triggering events across PNG during MAM is associated with the widespread dominance of deep convection induced by the north-westerly monsoon. Both the central cordillera and areas of lower elevation are affected by landsliding, during the wetter season, due to the increase in water availability and the interaction of this water with a larger number of potentially susceptible slopes. During MAM therefore, rainfall is the less dominant process determining the spatial variability of landsliding, as the vast majority of the region experiences high rainfall accumulations during this time. It is likely therefore, that underlying landslide

susceptibility is the more dominant process determining the spatial distribution of landslides during this season.

4 Discussion

In this study, the methods used to generate a spatial and temporal landslide inventory for the sparse data region of PNG have been outlined and the occurrence of landslide-triggering events between 1970 and 2013 have been examined. The development of landslide inventories is frequently challenging due to the nature of landslide events, as outlined at the start of this article. It is fully recognised that the newly developed PNG landslide database underestimates the true numbers of landslides which occur in PNG and that although we have used a number of techniques to reduce spatial and temporal uncertainty, that error levels remain quite large. For example, the uncertainty around the true numbers of landslides associated with entries in the database can be illustrated in Fig. 11. As only those entries where dates and locations could be identified with reasonable accuracy were included in the database, many individual landslide deposits associated with a specific triggering-event had insufficient attribute information (i.e. identifiable spatial references) to be individually entered into the inventory. Much of the uncertainty identified in Fig. 11, is linked to the type of landslide-triggering event. Frequently, earthquake events which resulted in landslides had sufficient information to identify an area where the majority of landslides associated with the earthquake occurred. There was however insufficient information to provide entries for individual landslides triggered by the earthquake, unless they were of particular size or had specific, note-worthy socio-economic impacts (e.g. Bairaman Landslide in New Britain, May 1985; King and Loveday, 1985). In these instances, a single database entry represents all the individual landslides which were triggered by the earthquake. The findings from the database indicate that earthquakes and flooding generate the greatest uncertainty with regard to the "true" numbers of landslides triggered, while individual landslides associated with mining and rainfall events (which did not result in flooding)

are generally better documented. This is largely due to landslides being categorized as secondary hazards to earthquakes or flooding which are the primary hazards. In such cases the spatial and temporal information related to landslides is very poor.

As noted in Sect. 2.1 the timing of many landslides is uncertain, particularly where there are no eye witness accounts to the event. To capture this uncertainty and constrain the landslide event for comparison with rainfall climatology data, the time of initiation was approximated using a minimum and maximum date boundary relating to the earliest and latest dates within which the landslide event occurred. These dates generally relate to the start and end dates of potential landslide-triggering events, such as a flood event. Landslides were then grouped by month (Figs. 5 and 6) or season (Figs. 7 and 10) using the end date information. This has the potential to introduce errors where landslides are assigned to a month or season which does not correspond to its time of actual initiation. In turn, this could mean that a landslide-triggering event is not being compared against the correct rainfall climatology data and that patterns of activity associated with a specific season may be over or under-represented based on the bias introduced by using this metric. Although this cannot be ruled out completely, it has been possible to determine that 80 % of all landslide entries in the database are constrained within a 10 day period or less. This means that the vast majority of landslides were initiated over a defined 10 day (or less) period and therefore we can be confident that these events are assigned to the correct 3- or 6-monthly season in the majority of cases. There is slightly more uncertainty for events assigned to monthly timescales, as where 10 day periods cross from one month into the next, the latest month will always be used. Towards the end of the wetter season, the numbers of flood-associated trigger mechanisms tends to increase and the number of days between the minimum and a maximum date boundaries also tends to increase. We believe that this helps to explain the second peak in rainfall-associated, landslide-triggering events observed in May (Fig. 5), which is more traditionally seen as a period of transition as the north-westerly monsoon period wanes and the south-easterly trade flows become more dominant.

In spite of the limitations described above, we believe that this new, national-scale landslide inventory accurately captures those high-impact landslides which contribute to the majority of landslide fatalities and damage. As these are the types of landslide events which we would ideally like to mitigate against in the future, understanding how, when and where these events occur across space and time is very valuable. The findings illustrate that these landslides are strongly controlled by the annual north-westerly monsoon cycle and that during different phases of the seasonal cycle landslides are potentially triggered by very different magnitudes of rainfall (Fig. 6). Future research would hope to assess the long term trends in landslide activity at a regional-scale and assess how these changes are linked to changes in the climate, the strength of the monsoon cycle and ENSO. In order to do this effectively, continued development of the database and a more systematic approach to landslide recording is essential, so that this type analysis can be extended.

5 Conclusion

Regional-scale landslide inventories offer a greater understanding of the temporal and spatial distribution of landslide events, their characteristics and triggers. In this study we have constructed the first, regional-scale landslide inventory for PNG, bringing together a range of existing and new datasets to form a single, commonly formatted database of landslide entries. Whilst the challenges involved in the development of the database have been described in detail, we believe that the database constitutes a significant advance in knowledge and data that can be used by researchers and planners alike. Analyses of the newly collated landslide inventory demonstrates how this information can be used to understand regional-scale, spatial and temporal variability and the relationships between landslides and different trigger factors. The key findings from this research are:

- Rainfall and the various combinations of triggers associated with it, account for the majority (~ 61 %) of all medium to large landslide-triggering events in the PNG inventory.
- There is also a strong climatic control on the landslide-triggering events, with greater numbers being observed between December and March, with a second peak in May, and fewer observed between June and October. This relates closely to periods dominated by north-westerly monsoon flows and south-easterly trade flows respectively.
- The majority of landslides initiated in the drier season are linked to extreme rainfall (~ 61 %), while landslides initiated during the wetter season can be triggered during months with lower absolute rainfall totals.
- In addition, there is large year to year variability in the annual occurrence of landslide events and this can be linked to different phases of ENSO. Landslide-triggering events continue to occur throughout north-westerly monsoon seasons in all phases of ENSO, but fewer numbers are observed during drier season months of El Niño phases, than either La Niña or ENSO neutral phases.
- The spatial distribution of landslide-triggering events is primarily determined by a combination of relief, precipitation and population density.

The information collected and analysed in this study contributes to the first country-wide assessment of landslides which result in fatalities and significant damage. Based on this analysis, landslide hazard hotspots and relationships between landslide occurrence and rainfall climatology can be identified. This information can prove important and valuable in the assessment of trends and future behaviour, which can be useful for policy makers and planners.

Acknowledgements. This research was jointly supported by the Met Office, University of Leicester and the University of Papua New Guinea. Special thanks go to colleagues at the PNG Mineral Resources Authority (MRA) and the Department of Mineral Policy and Geohazards Management in Papua New Guinea for their help and support throughout the completion of this research.

References

Adler, R. F., Huffman, G. J., Chang, A., Ferraro, R., Ping-Ping Xie, Janowiak, J., Rudolf, B., Schneider, U., Curtis, S., Bolvin, D., Gruber, A., Susskind, J., Arkin, P. And Nelkin, E.: The Version 2 Global Precipitation Climatology Project (GPCP) monthly precipitation analysis (1979–present), J. Hydrometeorol., 6, 1147–1167, 2003.

Anton, L. and Gibson, G.: Analysing earthquake hazard in Papua New Guinea, in: Proceedings of the Australia Earthquake Engineering Society Conference, Ballarat, Australia, availalbe at: http://www.aees.org.au/wp-content/uploads/2013/11/14-Anton.pdf (last access: 6 August 2015), 2008.

Blong, R. J.: Mudslides in the Papua New Guinea Highlands, in: Proceedings of the 4th International Conference and Field Workshop on Landslides, Tokyo, Japan, 1985.

Blong, R. J.: Natural hazards in the Papua New Guinea highlands, Mt. Res. Dev., 6, 233–246, 1986.

Bourke, R. M. and Harwood, T. (Eds): Food and Agriculture in Papua New Guinea, ANU E Press, The Australian National University, Canberra, Australia, 38–45, 2009.

Brakenridge, G. R.: Global Active Archive of Large Flood Events, Dartmouth Flood Observatory, University of Colorado, available at: http://floodobservatory.colorado.edu/Archives/index.html (last access: 8 July 2015), 2010.

Brakenridge, G. R. and Karnes, D.: The Dartmouth Flood Observatory: an electronic research tool and electronic archive for investigations of extreme flood events, Geological Society of 25 America Annual Meeting, Geoscience Information Society Proceedings, Denver, USA, 1996.

Center for International Earth Science Information Network – CIESIN – Columbia University, International Food Policy Research Institute – IFPRI, The World Bank, and Centro Internacional de Agricultura Tropical – CIAT, Global Rural-Urban Mapping Project, Version 1

(GRUMPv1): Population Density Grid, NASA Socioeconomic Data and Applications Center (SEDAC), Palisades, NY, doi:10.7927/H4R20Z93, 2011.

Comegna, L., Picarelli, L., and Urciuoli, G.: The mechanics of mudslides as a cyclic undrained-drained process, Landslides, 4, 271–232, 2007.

EM-DAT: The OFDA/CRED International Disaster Database, Université Catholique de Louvain, Brussels, Belgium, available at: http://www.em-dat.net, last access: 14 May 2015.

Greenbaum, D., Tutton, M., Bowker, M. R., Browne, T. J., Greally, K. B., Kuna, G., McDonald, A. J. W., Marsh, S. H., Northmore, K. J., O'Connor, E. A., and Tragheim, D. G.: Rapid methods of landslide hazard mapping: Papua New Guinea case study, British Geological Survey Technical Report WC/95/27, British Geological Survey, Nottingham, UK, 1995.

Guha-Sapir, D. and Below, R.: The quality and accuracy of disaster data – a comparative analysis of three global data sets, Working paper prepared for the Disaster Management Facility, World Bank, CRED, Brussels, available at: www.cred.be/sites/default/files/Quality_accuracy_disaster_data.pdf (last access: 14 May 2015), 2002.

Guzzetti, F., Peruccacci, S., Rossi, M., and Stark, C. P.: Rainfall thresholds for the initiation of landslides in central and southern Europe, Meteorol. Atmos. Phys., 98, 239–267, 2007.

Hill, K. C. and Hall, R.: Mesozoic-Cenozoic evolution of Australia's New Guinea margin in a west Pacific context, in: Defining Australia: The Australian Plate, edited by: Hillis, R. and Müller, R. D., Geol. Soc. Australia Spec. Pub. 22 and GSA Spec. Paper 372, Goelogical Society of America, Boulder, Colorado, 259–283, 2003.

Hovius, N., Stark, C. P., Tutton, M. A., and Abbott, L. D.: Landslide-driven drainage network evolution in a pre-steady-state mountain belt: Finisterre Mountains, Papua New Guinea, Geology, 26, 1071–1074, 1998.

Iverson, R. M.: Landslide triggering by rain infiltration, Water Resour. Res., 36, 1897–1910, 2000.

Keefer, D. K.: Investigating landslides caused by earthquakes – a historical review, Surv. Geophys., 23, 473–510, 2002.

King, J. and Loveday, I.: Preliminary geological report on the effects of the earthquake of 11th May 1985 centred near Biallo, West New Britain, Geological Survey of Papua New Guinea Report 85/12, Geological Survey of Papua New Guinea, Port Moresby, 1985.

Kirschbaum, D. B., Adler, R., Hong, Y., and Lerner-Lam, A.: Evaluation of a preliminary satellite-based landslide hazard algorithm using global landslide inventories, Nat. Hazards Earth Syst. Sci., 9, 673–686, doi:10.5194/nhess-9-673-2009, 2009.

Kirschbaum, D. B., Adler, R., Hong, Y., Hill, S., and Lerner-Lam, A.: A global landslide catalog for hazard applications: methods, results and limitations, Nat. Hazards, 52, 561–575, 2010.
Kuna, G.: The impact of landslides on national highways in the Highlands Region, Papua New Guinea Geological Survey Technical Note TN 8/98, Port Moresby, Papua New Guinea, 1998.
McAlpine, J. R., Keig, G., and Falls, R.: Climate of Papua New Guinea, Commonwealth Scientific and Industrial Research Organization, Canberra, Australia, 1983.
McGregor, G. R.: An assessment of the annual variability of rainfall: Port Moresby, Papua New Guinea, Singapore, J. Trop. Geogr., 10, 43–54, 1989.
McGregor, G. R. and Nieuwolt, S.: Tropical Climatology, An Introduction to the Climates of the Low Latitudes, 2nd Edn., Wiley and Sons, Chichester, 1998.
Meunier, P., Hovius, N., and Haines, A. J.: Regional patterns of earthquake-triggered landslide and their relation to ground motion, Geophys. Res. Lett., 34, L20408, doi:10.1029/2007GL031337, 2007.
Ota, Y., Chappell, J., Beryyman, K., and Okamoto, Y.: Late quaternary paleolandslides on the coral terraces of Huon Peninsula, Papua New Guinea, Geomorphology, 19, 55–76, 1997.
Pain, C. F. and Bowler, J. M.: Denudation following the November 1970 earthquake at Madang, Papua New Guinea, Z. Geomophol., Suppl. Bd., 18, 92–104, 1973.
Peart, M.: The Kaiapit Landslide: events and mechanisms, Q. J. Eng. Geol. Hydroge., 24, 399–411, 1991a.
Peart, M.: Ok Tedi mining project: site visit 29 April to 2 May 1991, Papua New Guinea Geological Survey Technical Note TN 12/91, Port Moresby, Papua New Guinea, 1991b.
Peart, M.: The geology and geotechnical properties of Chim Formation mudstones of Papua New Guinea, Papua New Guinea Geological Survey Technical Report 4/91, Papua New Guinea Geological Survey, Port Moresby, Papua New Guinea, 1991c.
Petley, D., Crick, W. O., and Hart, A. B.: The use of satellite imagery in landslide studies in high mountain areas, in: Proceedings of the Asian Conference on Remote Sensing, Kathmandu, Nepal, available at: http://a-a-r-s.org/aars/proceeding/ACRS2002/Papers/HMD02-9.pdf (last access: 6 August 2015), 2002.
Petley, D., Hearn, G. J., Hart, A., Rosser, N. J., Dunning, S. A., Oven, K., and Mitchell, W. A.: Trends in landslide occurrence in Nepal, Nat. Hazards, 43, 23–44, 2007.
Petley, D.: Global patterns of loss of life from landslides, Geology, 40, 927–930, 2012.
Qian, J.-H.: Why precipitation is mostly concentrated over islands in the maritime continent, J. Atmos. Sci., 65, 1428–144, 2008.

Ramage, C. S.: Role of a tropical “Maritime Continent” in the atmospheric circulation, Mon. Weather Rev., 96, 365–370, 1968.
Saunders, J.: Agricultural Land Use of Papua New Guinea: Explanatory Notes to Map, PNGRIS Publication No. 1, AIDAB, Canberra, 1993.
Stead, D.: Engineering geology in Papua New Guinea, Eng. Geol., 29, 1–20, 1990.
Tutton, M. A. and Kuna, G.: An appraisal of the condition and stability of the Highlands Highway, Papua New Guinea Geological Survey Report 95/1, Papua New Guinea Geological Survey, Port Moresby, Papua New Guinea, 1995.
Vohora, V. K. and Donoghue, S. L.: Application of remote sensing data to landslide mapping in Hong Kong, in: Proceedings of the XXth ISPRS Congress, Istanbul, Turkey, available at: http://www.isprs.org/proceedings/XXXV/congress/comm4/papers/398.pdf (last access: 6 August 2015), 2004.
Zeriga-Alone, T., Whitmore, N., and Sinclair, R.: The Hindenburg Wall: A Review of Existing Knowledge, Wildlife Conservation Society Papua New Guinea Program, PNG, Goroka, 7 pp., 2012.
Zêzere, J. L., Trigo, R. M., and Trigo, I. F.: Shallow and deep landslides induced by rainfall in the Lisbon region (Portugal): assessment of relationships with the North Atlantic Oscillation, Nat. Hazards Earth Syst. Sci., 5, 331–344, doi:10.5194/nhess-5-331-2005, 2005.

Table 1. Critical and relevant information obtained for each landslide entry in the new PNG landslide inventory.

Critical information collected in the database:	
Date	day.month.year/month.year
Location	Village, town or landmark
Province	Administrative province name
Relevant information collected in the database:	
Landslide Triggering Event (LTE) start date	Day Month Year
Landslide Triggering Event (LTE) end date	Day Month Year
LTE Duration in days	
Colloquial landslide name	
River/Catchment	
Landslide or landslide cluster location coordinates	*X* – Lat *Y* – Long
Number of landslides	
Landslide cluster group	0–10 I 10–100 I 100–1000 I > 1000
Landslide type	
Landslide volume (combined or single landslide)	
Landslide affected area (combined or single landslide)	
Trigger/Event Descriptor	
Earthquake Date	day.month.year
Earthquake coordinates	*X* – Lat *Y* – Long
Earthquake Magnitude	
Earthquake Depth (km)	
Impacts of the landslide/landslide cluster	
Scientific/journal publication reference	
PNG MRA or DMPGM report reference	
Disaster Identifier reference (GLIDE, EM-DAT disaster No.)	
Media reference	
Humanitarian response reference	

Table 2. Typical DN value ranges, for each wavelength, indicative of active landslides (Petley, 2002).

Band number	Wavelength (micrometers)	DN values of active landslides
1	0.45–0.515	60–100
2	0.525–0.605	60–100
3	0.63–0.69	50–120
4	0.75–0.90	70–130
5	1.55–1.75	80–140
6	10.40–12.5	140–190
7	2.09–2.35	60–110

Table 3. Return period in years for magnitude 6.0 earthquakes for selected tectonic seismic zones in PNG (Ripper and Letz, 1993).

Seismic zone	Seismic zone area (km^2)	Return period (yr) for magnitude 6.0 earthquake
Papuan Fold Belt	129 600	5.7
North Sepik	67 900	3.3
Ramu	86 400	1.9
Huon	40 100	1.9
New Britain	92 600	0.4
Bougainville Island	104 900	0.4

Table 4. La Nina and El Nino years identified from bimonthly MEI ranks (based on data sourced in 2012).

La Niña years	El Niño years
1970–1971	1972–1973
1973–1976	1982–1983
1988–1989	1986–1987
1999–2001	1991–1992
2007–2009	1994–1995
	1997–1998

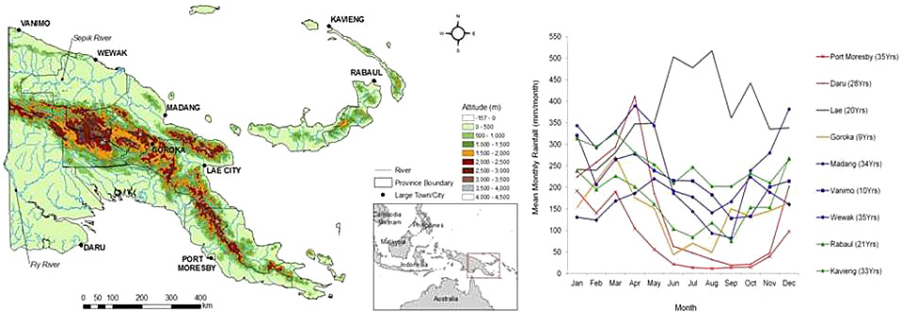

Figure 1. Location and geomorphology map of Papua New Guinea (PNG). The large towns/cities shown are also the location of World Meteorological Organization (WMO) rainfall gauge stations.

Figure 2. Photographs of landslides which have occurred in PNG: **(a)** debris flow near Dakgaman Village, Morobe Province; **(b)** Bolovip Mission, Western Province; **(c)** back-scarp of a rotational soil slump at Gera village, Chimbu Province. Photographs courtesy of the MRA.

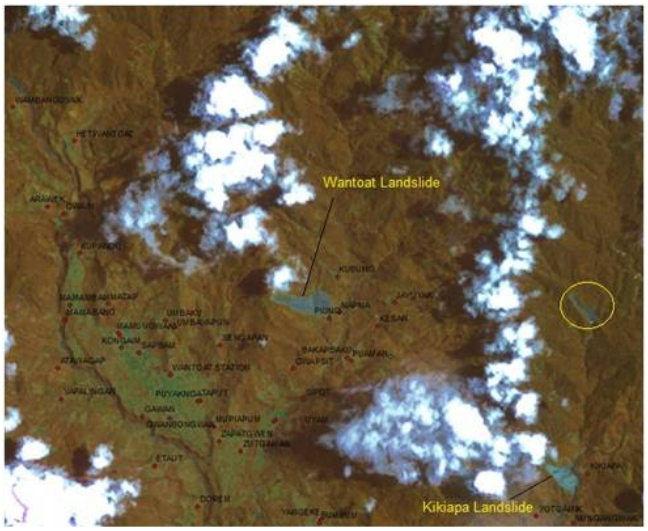

Figure 3. FCC 457 ETM+ image, acquired on 21 September 2002, showing the Wantoat, Kikiapa and Dakgaman (circled) landslides.

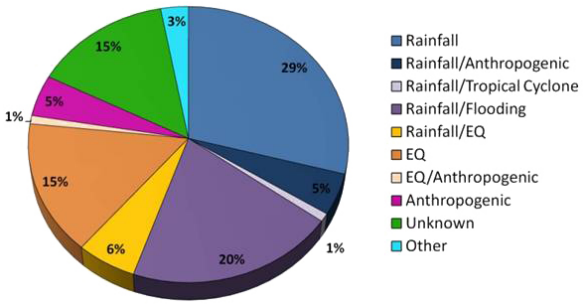

Figure 4. Distribution of landslide-triggering event types associated with landslides and landslide clusters recorded in the PNG landslide inventory between 1970 and 2013.

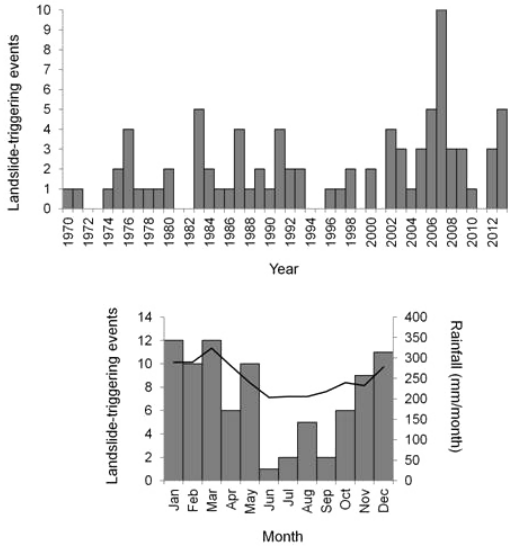

Figure 5. Annual occurrences of landslide-triggering events between 1970 and 2013 (top panel) and frequency of landslide-triggering events by month compared with monthly rainfall climatology based on 53 GPCC grid squares and reference period 1970–2010 (bottom panel).

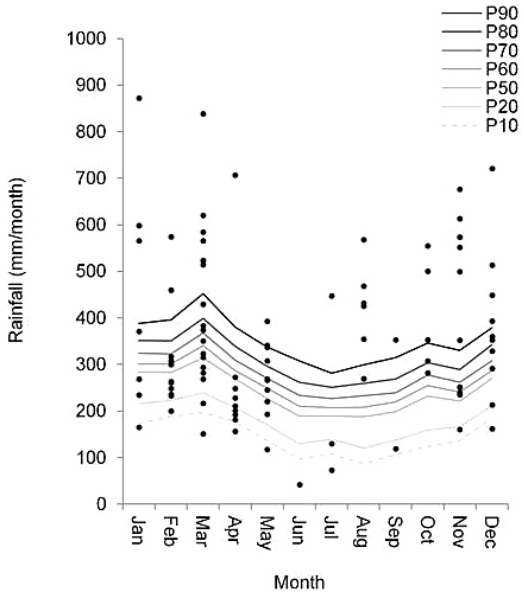

Figure 6. Percentiles of monthly precipitation calculated based on the 53 GPCC grid squares representing landslide affected areas in PNG (1970–2010) and landslide-triggering events.

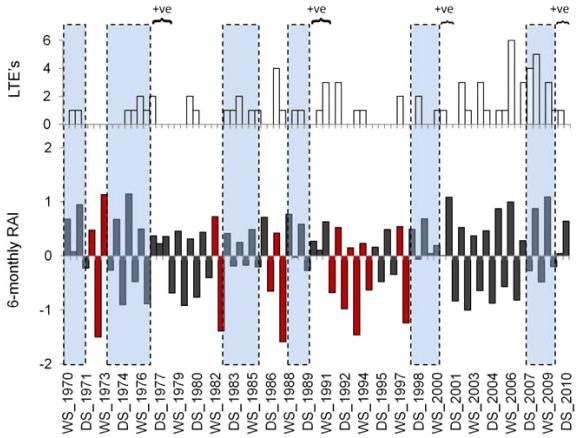

Figure 7. Bar charts show 6-monthly landslide-triggering events (white bars, top plot) and the corresponding 6-monthly rainfall anomaly index (grey bars, bottom plot). La Niña episodes are shown by the shaded blue columns, while consecutive 6-monthly periods with positive departures from the mean are identified by the "+ ve" labels. Seasons associated with El Niño are shown by the red bars.

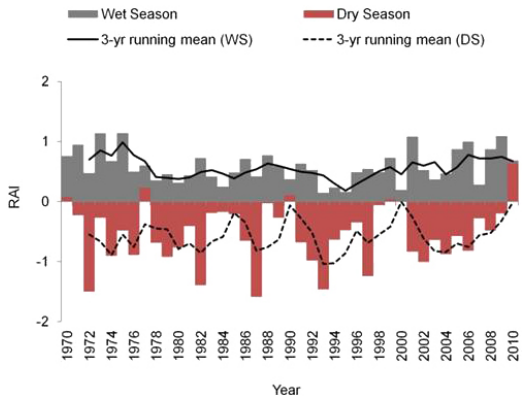

Figure 8. Comparison between wet season 6-monthly rainfall anomaly index and dry season 6-monthly rainfall anomaly index.

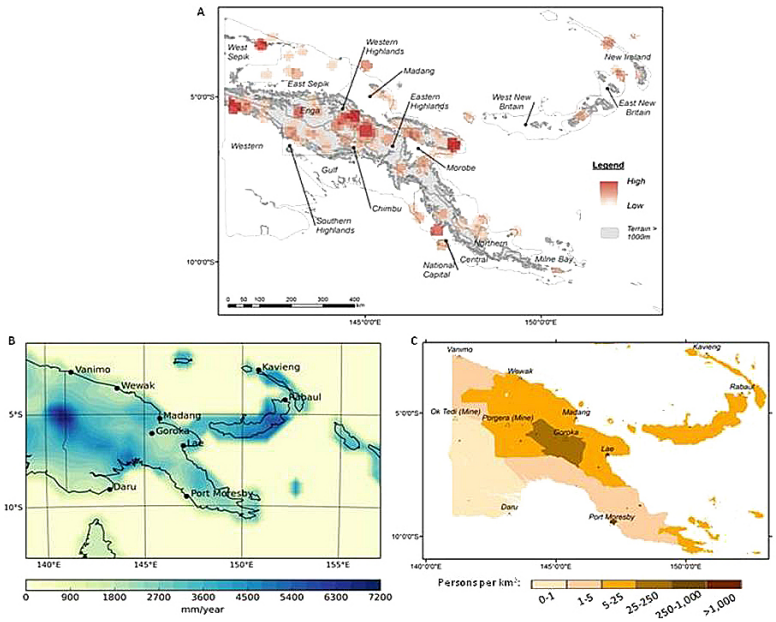

Figure 9. (a) The distribution of landslide entries between 1970 and 2013 shown as the density of latitude/longitude points around each 10 km^2 cell using a neighbourhood radius of 30 km. **(b)** The corresponding distribution of mean annual precipitation calculated over the period 1970 to 2010. **(c)** Population density measured as the number of persons per square kilometre of land area with a grid resolution of 30 arcsec (data produced by the Global Rural-Urban Mapping Project (GRUMPv1) and made available by the Center for International Earth Science Information Network (CIESIN)).

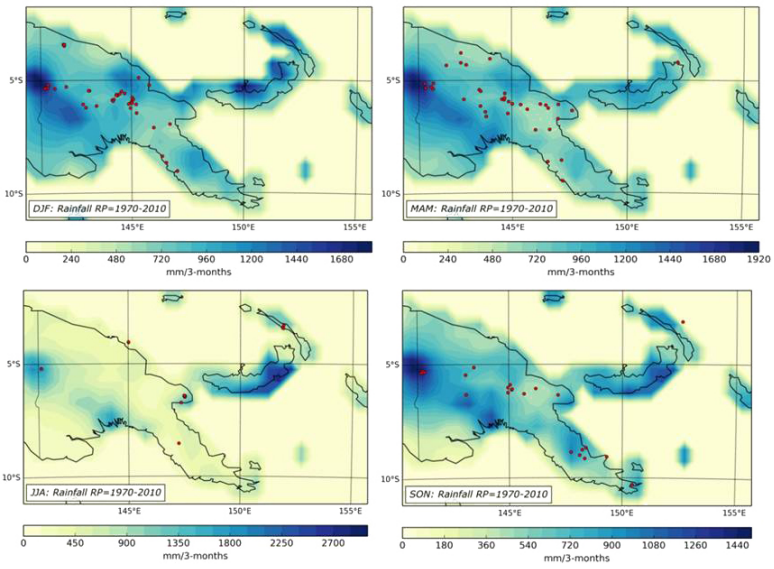

Figure 10. Seasonal composites of 3-monthly rainfall based on the 41 year reference period (RP) with all landslide entries linked to rainfall trigger mechanisms (1970–2013) overlain and shown by season using red dots.

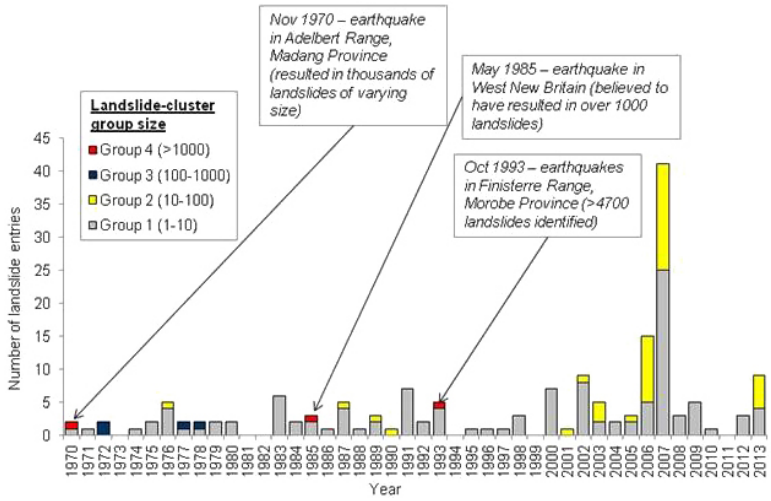

Figure 11. Landslide entries in the PNG landslide inventory showing the temporal distribution of events and the uncertainty in total numbers of landslides associated with each entry.